Bulg. J. Phys. **37** (2010) 37–47

Studies on the Variations of ELF Atmospherics over Kolkata

S.S. De[1], **B.K. De**[2], **B. Bandyopadhyay**[1], **G Guha**[1], **S. Paul**[1], **A. Bhowmick**[2], **D.K. Haldar**[1], **G. Chattopadhyay**[2], **M. Sanfui**[1]

[1]S.K. Mitra Centre for Research in Space Environment, Centre of Advanced Study in Radio Physics and Electronics, University of Calcutta, Kolkata 700 009, India

[2]Department of Physics, University of Tripura, Agartala 799 130, India

Received *March 7, 2010*

Abstract. The atmospheric radio noise field strength (ARNFS) at 700 Hz and 2100 Hz over Kolkata (Lat. 22.56° N, Long. 88.5° E) exhibits various characteristic patterns of diurnal and seasonal variations. Some distinctive features at these two frequencies have been observed in respect of the level of ARNFS during all the months, the fall of level from nighttime to daytime value, the correlation in sunrise time and the role of cloud activity upon the seasonal maximum. The outcome of analysis of the recorded data will be presented in this paper.

PACS number: 92.60.Ry, 92.60.Wc, 92.60.Nv

1 Introduction

The lightning discharge current flows from cloud to ground (CG) or within the Intra-cloud (IC). These currents generate transient radio pulses termed as atmospherics or sferics. The flash of lightning lasts about 0.2 s, which is comprised of several strokes separated by about 50 to 60 ms and lasting for a few to tens of milli-seconds. The energy of electromagnetic radiation from lightning is spread over a frequency domain from a few hertz to several megahertz [1,2]. However, by virtue of the time scale of the return stroke, most of the energy is confined in the very low frequency (VLF: 3–30 kHz) and extremely low frequency (ELF: 3–3000 Hz) bands [3]. Originating from lightning activity, ELF energy is reflected by the lower ionosphere and the Earth's surface. It then propagates in a guided fashion between Earth-ionosphere boundaries which form a waveguide.

ELF sferics are mainly produced from the joint contributions of the vertical component of IC discharges and intra-cloud portions of CG discharges [4]. It is known that IC strokes have much longer discharge path, i.e., larger current moments where sufficient ELF sferics are produced [5].

South Africa, Central and South America, and South Eastern Asia are the main centers of global lightning activities. Characteristics of thunderstorm activities are very much dependent on the geographic location, local meteorological and seasonal conditions. Sferics which are the transient radio pulses generated from lightning discharge currents have important significance in regard to electrical phenomena occurring in different types of clouds during meteorologically active periods. During clear periods, atmospheric radio noise field strength (ARNFS) measurement provides the study of ionospheric propagation. Because of privileged geographical position of Kolkata (Lat. 22.56° N, Long. 88.5° E), one can study ARNFS from cloud discharge. Moreover, measurements of atmospherics at Kolkata in the ELF band were not performed earlier. To elucidate it, ELF atmospherics over Kolkata are being recorded continuously since 1995. Some observational results of atmospherics and distinctive features of ARNFS at ELF band at frequencies 700 Hz and 2100 Hz will be presented in this paper. The attenuation of ELF is large in the selected frequencies [4,6]. So, the present observations will be confined to the nearer sources mainly on Bay of Bengal and North-East (hilly region) part of India. The aim is to investigate seasonal variation of ARNFS due to nearby cloud activity. It is significant that one frequency 2100 Hz is included in the range of transverse resonance frequencies of the Earth-ionosphere cavity. The transverse resonances are caused in the Earth-ionosphere cavity by multiple reflections between the Earth and ionosphere. The first resonance falls in the range of 1600-2500 Hz which may be excited by lightning discharges [7]. This kind of effect may be explored up to 1000 km.

2 Experimental Set Up

An inverted-L type antenna is used to receive the vertically polarized atmospherics at ELF band. The voltage induced at the antenna was fed to the input of a radio frequency receiver tuned at 700 Hz and 2100 Hz via low-pass filters. Each receiver is consisted of two tuned-voltage stages followed by high input impedance unit gain buffer. The output of the buffer is detected and further amplified by quasi-log DC amplifier. Using computer sound card, data are recorded at a sample rate of 10/s which have been analyzed through Origin 7.0. An automatic gain control circuit is used to increase the dynamic range of the amplifier.

3 Analysis of the Observational Results

Recording of ARNFS at 700 Hz and 2100 Hz are being carried out continuously over Kolkata. The data exhibited a number of characteristic features. In Figure 1, a sample record of September 12, 2007, is shown which depicts some typical

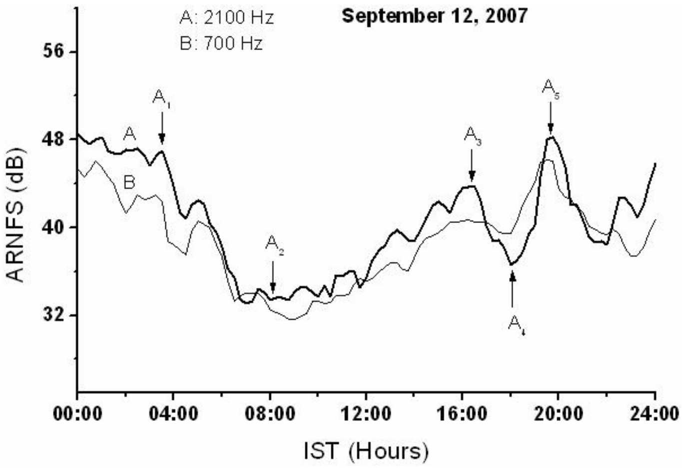

Figure 1. A typical record of diurnal variation of ARNFS at 700 Hz and 2100 Hz as observed over Kolkata on September 12, 2007, showing sunrise effect (A_1), morning minimum (A_2), afternoon maximum (A_3), sunset minimum (A_4), and night-time maximum (A_5). Y-axis depicts the ARNFS in terms of induced voltage in dB above 1 μV.

characteristics of ARNFS over Kolkata. These are: (i) sunrise effect (A_1), (ii) morning minimum (A_2), (iii) afternoon maximum (A_3), (iv) sunset minimum (A_4), and (v) night-time maximum (A_5). The chances of occurrence of all these features are found to be about only once in a week.

Sunrise effect is the fall of ARNFS from nighttime higher value to lower daytime value following distinct steps in most of the days. Morning minimum may go across the cut-off level. It is observed that the afternoon maximum and sunset minimum are usually not sharp and less prominent in all days.

The monthly median values of diurnal variations of ARNFS averaged over three consecutive years at these two frequencies are depicted in Figure 2. It is seen from the different curves that the morning minimum is the lowest value of the day, called daily-minimum, $D_{\min}$, in the absence of major thunderstorm activities. Usually, the number of occurrence of daily minimum at the morning is comparatively higher during December to February whereas its occurrence number at the morning is small from June to September.

Figure 3 shows the monthly variations of the time of occurrence of $D_{\min}$ at 700 Hz and 2100 Hz together with monthly variation of local sunrise times. At 2100 Hz, $D_{\min}$ occurs almost around sunrise time in the months of January and February, where as, it is highly zig-zag in the case of 700 Hz.

The average value of daytime and nighttime amplitude level of ARNFS can be

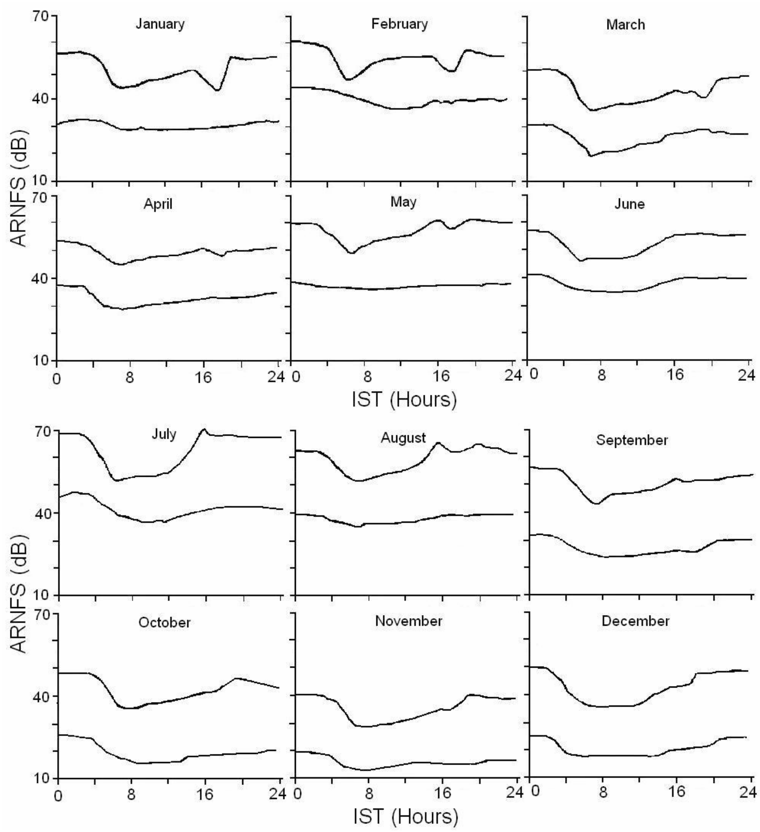

Figure 2. Monthly median values of diurnal variations of ARNFS in terms of induced voltage in dB above 1 μV over Kolkata for all the months. Upper curve: 2100 Hz, Lower curve: 700 Hz.

expressed as

$$\mathrm{A}_d = \frac{1}{\tau_1} \int (\sigma) E(t) dt, \tag{1}$$

and

$$\mathbf{A}_n = \frac{1}{\tau_2} \int (\sigma) \mathbf{E}(t) dt \tag{2}$$

where (σ) – the conductivity tensor of the medium and is given by

$$(\sigma) = \begin{pmatrix} \sigma_1 & -\sigma_2 & 0 \\ \sigma_2 & \sigma_1 & 0 \\ 0 & 0 & \sigma_0 \end{pmatrix} \tag{3}$$

σ_1 – Pedersen conductivity, σ_2 – Hall conductivity, $\sigma_0 = \sigma_1 + \dfrac{\sigma_2^2}{\sigma_1}$, – the Cowling

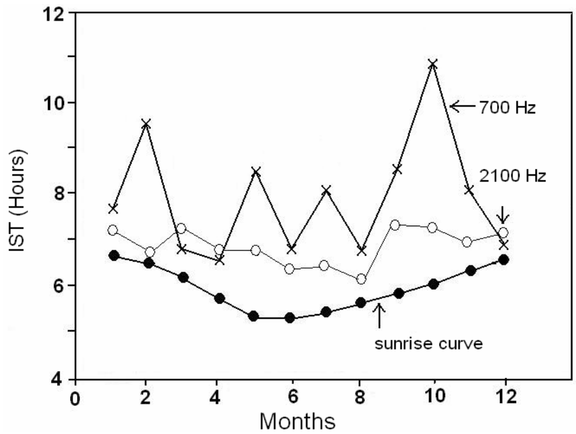

Figure 3. Month-to-month variations of time of occurrence of $D_{\min}$ at 700 Hz and 2100 Hz along with the sunrise time at the receiving station. Uppermost: 700 Hz; middle: 2100 Hz; lowest continuous: sunrise time.

conductivity, $E(t)$ – instantaneous level of ARNFS, τ_1 – time interval between a sunrise and a next sunset, and τ_2 is the time interval between a sunset and a next sunrise.

The geomagnetic field B_0 is assumed to be in the z-direction. For the upper D-region of the ionosphere, the form of the conductivity tensor for harmonic fields with time dependence $\sim e^{-i\omega t}$ is chosen in (3).

The values of A_d and A_n have been calculated for each day by using the area between ARNFS curve and time axis. The study of the variations of A_d and A_n from month-to-month for the two frequencies shows that both A_d and A_n are maximum in July and minimum in November. A_d = 49.5, A_n = 53.2 in July and A_d = 17.1 and A_n = 22.5 in November for 700 Hz. At 2100 Hz, A_d = 65.0, A_n = 67.3 in July and A_d = 29.3, A_n = 37.8 in November.

A small fade is observed in ARNFS around sunset, which is comparatively higher at 2100 Hz. The number of occurrence of sunrise minimum is higher compared to that of sunset minimum in all months. The number of sunset minimum is very small during June to September. A peak is observed around post-midday period of August and September at 2100 Hz. The peak is also observed around post-evening period during October to January at 2100 Hz but such peak was not prominent at 700 Hz. The maximum value of the level in a day is called as daily-maximum $D_{\max}$ which shows variation in the occurrence time in different months. It is seen that $D_{\max}$ occurs between 0000 to 0600 h during December to March. It occurs between 1800 to 2400 h during April-May and September-November, while $D_{\max}$ occurs between 1200 to 1800 h in June-August period. The average value of $D_{\max}$ is greater than almost 42 dB above

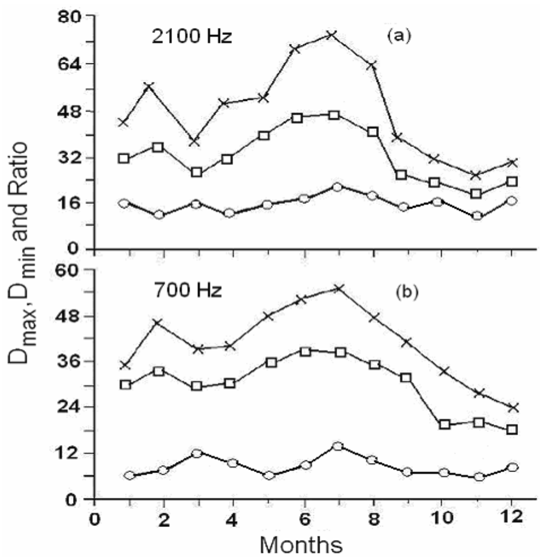

Figure 4. Month-to-month variations of $D_{\max}$ and $D_{\min}$ of ARNFS at two frequencies and the ratio $D_{\max}/D_{\min}$ (in dB the ratio appears as difference), where, (a) 2100 Hz and (b) 700 Hz.

1 μV throughout the day. Sometimes, it goes up to 65 dB value at the late evening time.

The levels of daily minimum $D_{\min}$, daily maximum $D_{\max}$ and their ratio in dB are shown in Figure 4. Both $D_{\max}$, $D_{\min}$ and the ratio are maximum in July and lowest in November. The ratio $D_{\max}/D_{\min}$ is also maximum in July both at 700 Hz and 2100 Hz. $D_{\max}/D_{\min}$ shows some smaller peaks in March and October at 2100 Hz, while the ratio shows larger value during March–April at 700 Hz.

From observations, the average rate of fall of ARNFS from nighttime value to the daytime minimum at these frequencies can be estimated. It is seen that at 2100 Hz, the average slope of fall is distinctly highest in July, whereas the slope is lowest during February and May.

The seasonal variation of $D_{\min}$, $D_{\max}$ and their ratio at 2100 Hz and 700 Hz are shown in Figure 5. Both $D_{\max}$ and $D_{\min}$ are found to be highest in monsoon time (June 15-September 15) and lowest in post-monsoon time (September 16-November 30). Also, the ratio $D_{\max}/D_{\min}$ in dB is maximum in monsoon at 2100 Hz and in post-monsoon at 700 Hz. The values of $D_{\max}$ and $D_{\min}$ are almost same in winter (December-February) and pre-monsoon (March–June 15).

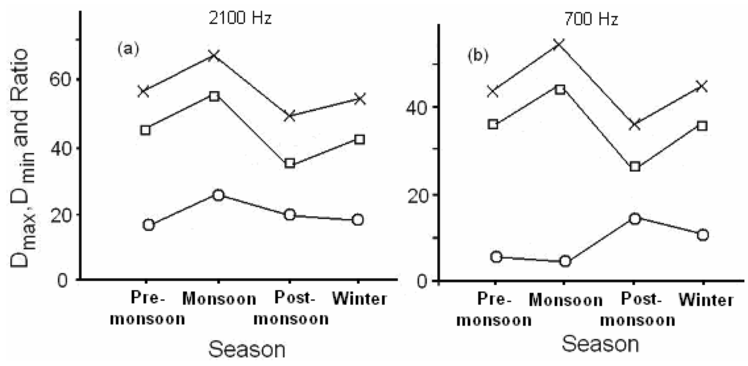

Figure 5. Seasonal variations of $D_{\max}$, $D_{\min}$ and $D_{\max}/D_{\min}$ at 2100 Hz and 700 Hz are shown here. The curves at the top and middle in both (a) and (b) depict $D_{\max}$ and $D_{\min}$, while the bottom graphs in (a) and (b) represent the ratio: $D_{\max}/D_{\min}$.

4 Discussion

ARNFS is known to have intimate connection with different types of lightning during thunderstorms. The most common sources of lightning is the electric charge separation in ordinary thunderstorm cloud. The main lightning discharges occur within the thunderstorm cloud (intra-cloud discharges) and cloud-to-ground discharges. The present result shows that ARNFS is higher at 2100 Hz than at 700 Hz. This is due to the fact that ELF waves received here are not from far sources greater than 800–1000 km. Conventional vertical field is highly attenuated over this distance [8]. Since the first transverse resonance frequency is in the range between 1600–2500 Hz, the ARNFS is higher at 2100 Hz.

Severe cloud activity occurs in the latitude of the present observing station during monsoon months. This is followed by larger values in $D_{\max}$ and $D_{\min}$ during monsoon compared to other seasons. During fair weather, contributions to ARNFS by the distant sources would dominate over nearer sources. The electromagnetic radiations from distant sources reach the receiver through ionospheric reflection from the heights 70 km at the daytime and 90 km at the nighttime [9]. Distant atmospherics are reflected from 90 km before sunrise. The region lower than 90 km acts as attenuator due to the presence of electrons of very low density. Electron density below 90 km after sunrise gradually increases due to decrease of solar zenith angle and for this, absorption also increases and goes on increasing until the formation of D-region is completed. Then the ELF radio waves are reflected from the region of smaller reflection coefficient at a height which is lower than 90 km. This presumes sunrise effect and $D_{\min}$ is obtained following ionospheric sunrise. In the present observation, sunrise minimum at 2100 Hz during December, January and February have been observed around local sunrise time. This ascertains that the lightning sources during December, January and February are mostly distributed in the north-south direction. In fact, the propagation of ELF and VLF radio waves are explained by waveguide mode theory [10]. The main deciding factor is the reflection height on which conductivity parameter depends. The difference in occurrence time of $D_{\min}$ at 2100 Hz and 700 Hz is due to different reflection heights at these two frequencies. The 2100 Hz is a frequency close to the lower range of VLF and is reflected from about 70 km at the day and 90 km at the night. During sunrise, modal conversion and interference between different modes are the causes of $D_{\min}$ [11]. The frequency 700 Hz corresponds to wavelength of the order of 430 km. As the wavelength of 700 Hz is three times longer than that of 2100 Hz, it is expected that the former can penetrate deeper into the ionosphere. Or, in other words, the reflection height for 700 Hz may be higher than that for VLF [12,13]. The radio wave at 2100 Hz, though within the spectrum of ELF, is close to the lower end of VLF band and it may be treated to be reflected from D-region where electron collision frequency plays an important role in the expression for refractive index. But radio wave at 700 Hz may be assumed to be reflected at a height above D layer, and here the gyro-frequency term dominates over the collision frequency term in the expression for refractive index. The normal reflection height of electromagnetic wave in the ionosphere varies with frequency, with lower frequencies reflected at lower height where electron density is lower. The ordinary (O) and extra-ordinary (X) rays have their own polarization and index of reflection. The extra-ordinary ray is reflected weakly except by extreme sharp ionospheric gradients and therefore penetrates more deeply into the ionosphere [14,15]. In the case of propagation of 2100 Hz, thickness of D-region does not come in, whereas in the propagation of 700 Hz, thickness of the lower ionosphere is important. This is the main cause of irregularities in the time of occurrence of $D_{\min}$ at 700 Hz.

Out of total number of 916 days of record over a period of 3 years, number of missing sunrise effects are 462 at 700 Hz and 322 at 2100 Hz. Out of them, the missing sunrise effects are related to locally active days thunderstorms with overhead cloud and heavy rainfall. In this case, propagational radio noise field from distant sources is submerged by ARNFS from local cloud activity. Remaining days of missing sunrise effect, not related to any local cloud activity, may be attributed to isotropic distribution of lightning sources about the receiving station. In this case, noise field should appear to be isotropically distributed about the receiving station. So, a sunrise at the ionosphere along a particular path can not produce appreciable effect in integrated ARNFS. It is worth mentioning that principal geomagnetic storm, solar flares are the other agents causing the disappearance of sunrise effect on long distance propagation field. Among missing sunrise effects, not related to local cloud activity, a good number of those are related to principal geomagnetic storms and solar flares. Extra ionization in the ionospheric D-region during solar and geomagnetically active days can give rise to flat nature in the record of ARNFS during local sunrise [16,17].

Cloud activities in eastern part of India and coastal belt of Bay of Bengal are very high in July and low in November. For this reason, the values of A $_d$ and A$_n$ during January and February is due to occurrences of lightning activity related to winter thunderstorm over the Bay of Bengal which is only a few hundreds of km from the receiving station.

The highest value of $D_{\max}/D_{\min}$ during monsoon is obvious due to wide variation of lightning activity over a complete day during this period. The larger values of ARNFS during March-April and November at 700 Hz are remarkable and it indicates that the rate of fall at this frequency is not controlled by source-activity but also by the characteristics of double layer propagation of ELF radio wave. It appears that two layer propagation at 700 Hz is good during March-April.

The highest rate of rise of ARNFS in July is the result of faster rise of cloud activity following the mid-day during this month. The peak in the rate of rise of ARNFS observed in March at 700 Hz may be due to the effect of transitional month.

It is expected that there is a transitional frequency near 1000 Hz such that, above this frequency, the variation of ARNFS is rhythmic and the variations are complex below that frequency due to involvement of double layer propagation.

5 Conclusion

Some specific observational aspects on the variations of ELF atmospherics from the analysis of the recorded data over Kolkata are presented here in terms of changes of ARNFS at 700 Hz and 2100 Hz. Although different theories are developed for ELF propagation through the ionospheric medium traversed by the geomagnetic field, which are generally utilized to explain various anomalies observed in ELF signal parameters in the lower ionosphere by man-made and natural events, still there are many outstanding problems which demand complete interpretations. Those may be cited as:

(i) The anomalous variations of ELF signal parameters crossing the nearby regions of high seismic activity several days prior and also later from the date of occurrence of large earthquakes;

(ii) During any accident to any Nuclear Power stations; the exact generation mechanism of ELF/VLF signals;

(iii) During high power high frequency electromagnetic wave propagation from ground transmitters, the exact non-linear interaction within the ionosphere [18-22];

(iv) Anomalies in the observed frequency shift in the first resonance mode of the Schumann spectra, while all other modes are almost stable;

(v) Correct explanation of the decrease in the first and second Schumann resonance modal frequencies during solar proton event, and increase in the first mode bandwidth during solar X-ray burst preceded by proton precipitation [23-26];

(vi) Anomaly to explain the exact connectivity between sprites, lightning and ELF waves [8,27-30].

In most of the theoretical analyses, D-region behaviour has not been taken into account in detail. Moreover, there are differences in the compositions between different heights at the Earth-ionosphere cavity, effects due to lateral ionospheric gradients [31,32], radial inhomogeneity, fluctuation of the near-Earth atmospheric layer conductivity, day-night asymmetry and local perturbations within the cavity are always existing which are not considered in detail in the formulations at large. Increase in atmospheric conductivity near the Earth leads to changes in the vertical electric current, which in turn owes to changes in ionospheric parameters [32]. Also, aeronomical factors and ionization mechanism by solar and galactic cosmic rays, meteorological parameters and also lithosphere-ionosphere interaction have not been taken appropriately in the formulation.

The present paper envisaged some peculiarities which have been discussed in this paper in terms of observational analyses of ELF waves. It is contemplated that the studies of ELF wave propagation from various perspectives will be successful to resolve different problems. From the present analyses, the observed results may be summarized as

(i) the level of ARNFS is higher at 2100 Hz compared to 700 Hz because of transverse resonance;

(ii) both $D_{\max}$ and $D_{\min}$ are higher in monsoon;

(iii) time of occurrence of $D_{\min}$ at 700 Hz exhibits irregular monthly variations due to involvement of double layer reflection at this frequency;

(iv) local thunderstorms and magnetic activity destroy the sunrise effect.

Acknowledgements

The authors gratefully acknowledge the financial support provided by Indian Space Research Organization (ISRO) through S K Mitra Centre for Research in Space Environment, University of Calcutta, Kolkata, India.

References

[1] C.D. Weidman, E.P. Krider (1986) *Radio Sci.* **21** 964.

[2] C.P. Bruke, D.E. Jones (1992) *J. Atmos. Terr. Phys.* **54** 243.
[3] S.A. Cummer, U.S. Inan (2000) *Radio Sci.* **35** 385.
[4] R. Barr, D.L. Jones, C.J. Rodger (2000) *J. Atmos. Sol. Terr. Phys.* **62** 1689.
[5] T.L. Teer, A.A. Few (1974) *J. Geophys. Res.* **79** 3436.
[6] S.A. Cummer (2000) *IEEE Trans. Anten. Propag.* **48** 1420.
[7] A.E. Reznikov, A.I. Sukhorukov, D.E. Edemskii, V.V. Kopeikin, P.A. Morozov, P.S. Ryabov, A.Yu. Shchekotov, V.V. Solov'ev (1993) *Antartic Sci.* **5** 107.
[8] S.A. Cummer, U.S. Inan, T.F. Bell, C.P. Barrington-Leigh (1998) *Geophys. Res. Lett.* **25** 1281.
[9] M. Hayakawa, S. Shimakura (1978) *Trans. Inst. Electrn. Comun. Eng. Jpn.* **E61** 15 1978.
[10] J.R. Wait (1982) *Electromagnetic waves in stratified medium*, Pergamon Press, Oxford, UK.
[11] K.J.W. Lynn (1973) *J. Atmos. Terr. Phys.* **35** 439.
[12] M. Yamashita (1967) *J. Atmos. Terr. Phys.* **29** 937.
[13] M. Yamashita (1969) *J. Atmos. Terr. Phys.* **31** 1049.
[14] R.A. Pappert, W.F. Moler (1978) *J. Atmos. Terr. Phys.* **40** 1031.
[15] S.A. Cummer, U.S. Inan (2000) *Radio Sci.* **35** 1437.
[16] G. Satori (1991) *J. Atmos. Terr. Phys.* **53** 325.
[17] R.H.W. Friedel, A.R.W. Hughes, R.L. Dowden, C.D.D. Adams (1993) *J. Geophys. Res.* **98** 1571.
[18] P.P. Belyaev, D.S. Kotik, S.N. Mityakov, S.V. Polyakov, V.O. Rapoport, V.Yu. Trakhtengerts (1987) *Radiophysics and Quantum Electronics* **30** 189.
[19] Y.N. Taranenko, U.S. Inan, T.F. Bell (1992) *Geophys. Res. Lett.* **19** 61.
[20] R. Barr, P. Stubbe (1984) *J. Atmos. Terr. Phys.* **46** 315.
[21] Yu.M. Yampolski, P.V. Bliokh, V.S. Beley, V.G. Ganlushko, S.B. Kascheev (1997) *J. Atmos. Terr. Phys.* **59** 335.
[22] P. Stubbe, H. Kopka, M.T. Rietveld, R.L. Dowden (1982) *J. Atmos. Terr. Phys.* **44** 1123.
[23] P.T. Verronen, Th. Ulich, E. Tnuruen, C.J. Rodger (2006) *Ann. Geophys.* **24** 187.
[24] V.C. Roldugin, Ye.P. Maltsev, A.N. Vasiljev, E.V. Vashenyuk (1999) *Ann. Geophys.* **17** 1293.
[25] V.C. Roldugin, Ye.P. Maltsev, A.N. Vasiljev, A.V. Shvets, A.P. Nikolaenko (2003) *J. Geophys. Res.* **108** 1.
[26] J. McGlade, H. Yang, V.P. Pasko (2004) *NSF EE REU PENN STATE Annual Research Journal* **2** 42.
[27] M. Stanley, M. Brook, P. Krehbiel, S.A. Cummer (2000) *Geophys. Res. Lett.* **27** 871.
[28] E. Huang, E. Willams, R. Boldy, S. Heckman, W. Lyons, M. Taylor, T. Nelson, C. Wong (1999) *J. Geophys. Res.* **104** 16943.
[29] Y. Hobara, N. Iwasaki, T. Hayashida, M. Hayakawa, K. Ohta, H. Fukunishi (2001) *Geophys. Res. Lett.* **28** 935.
[30] R.A. Marshall, U.S. Inan, T. Neubert, A. Hughes, G. Satori, J. Bor, A. Collier, T.H. Allin (2005) *Ann. Geophys.* **23** 2231.
[31] E.C. Field, R.G. Joiner (1982) *Radio Sci.* **17** 693.
[32] J.M. Fuks, R.S. Shubova (1994) *Geomag. Aeron.* **34** 229.